



Shvabyuk V. I., Rotko S. V., Ribeiro L. F., Kuts N. H., Zakharchuk V. I., Shvabyuk V. V. (2024). The problem of the reliability of bending models for composite plates of medium thickness. *Journal of Engineering Sciences (Ukraine)*, Vol. 11(1), pp. D36–D43. [https://doi.org/10.21272/jes.2024.11\(1\).d5](https://doi.org/10.21272/jes.2024.11(1).d5)

The Problem of the Reliability of Bending Models for Composite Plates of Medium Thickness

Shvabyuk V. I.^{1*}[0000-0002-1156-4405], Rotko S. V.¹[0000-0003-1860-7890], Ribeiro L. F.²[0000-0003-4336-6216], Kuts N. H.¹[0000-0003-1934-7189], Zakharchuk V. I.¹[0000-0002-5450-391X], Shvabyuk V. V.¹[0000-0001-8294-5291]

¹Lutsk National Technical University, 75, Lvivska St., 43018 Lutsk, Ukraine;

²Instituto Politécnico de Bragança, 253, Alameda de Santa Apolónia, 5300-252 Bragança, Portugal

Article info:

Submitted: August 25, 2023
 Received in revised form: January 9, 2024
 Accepted for publication: January 26, 2024
 Available online: February 7, 2024

*Corresponding email:

v.shvabyuk@gmail.com

Abstract. Most refined bending models of medium-thick plates, which consider transverse shear and partial compression deformations, differ little. However, despite a significant increase in the order of the governing differential equations, the results obtained from their equations give mainly a small increase in accuracy compared to the existing theories. On the other hand, such an increase in the order of the constructed systems of differential equations requires a significant increase in the effort required to solve them, complicates their physical interpretation, and narrows the range of people who can use them, primarily engineers and designers. Therefore, developing a plate-bending model that incorporates all the above factors and is on par with previously applied theories regarding the complexity of the calculation equations remains relevant. For example, most of the applied theories that do not consider transverse compression cannot be used to solve problems of contact interaction with rigid and elastic dies and bases because it is impossible to satisfy the conditions at the contact boundary of the outer surface of the plate, as well as the boundary conditions at the edges of the plate. Therefore, to provide guaranteed accuracy of the results, some researchers of these problems have introduced such a concept as “energy consistency” between the functions of representation of the displacement vector components, their number, the order of equations, and the number of boundary conditions. The authors, based on the developed version of the model of orthotropic plates of medium thickness, investigate the problem of taking into account the so-called “energy consistency” effect of the bending model, depending on the order of the design equations and the number of boundary conditions, as well as its usefulness and disadvantages in practical calculations. The equations of equilibrium in displacements and expressions for stresses in terms of force and moment forces are recorded. For rectangular and circular plates of medium thickness, test problems are solved, and the numerical data are compared with those obtained using spatial problems of elasticity theory, as well as the refined Timoshenko and Reissner theories. An analysis of the obtained results is provided.

Keywords: models of plate bending, orthotropic material, hypothesis method, plates of medium thickness, boundary conditions, normal stresses, self-equilibrium stress state.

1 Introduction

The many refined theories of plates and shells can be divided into two subgroups: one that uses the flat section hypothesis and the other where this hypothesis does not apply. The former is used to calculate thin shells and plates, and the latter is used to calculate shells and plates of medium thickness. This subgroup must consider not only transverse shear but also transverse compression, normal stress, and functions that consider the self-equilibrating stress states. Therefore, in this case, in

addition to the hypothesis method, there are several other theories of bending of medium-thickness plates that should be used in some instances of complex loads. At the same time, the refinements proposed by researchers must have a particular justification and be physically feasible.

In this work, based on the hypothesis method, the authors derive equilibrium equations for composite plates of medium thickness and formulae for normal stresses for some plate loads under various boundary conditions. Comparisons are made with the results obtained by more

accurate iterative methods of calculating plate bending or elasticity theory.

2 Literature Review

Currently, many refined models of bending plates made of isotropic and composite materials describe the stress-strain state of plates with greater or lesser accuracy compared to the classical Kirchhoff–Love theory.

These theories are described in detail in [1–3]. For shells, similar bending models are discussed in detail in a large review [4, 5]. The review of these theories usually begins with the elementary ones by Timoshenko [6] and Reissner [7] in the following form:

$$u = z\gamma_x; v = z\gamma_y; w = w(x, y), \quad (1)$$

where u, v, w – the components of the plate displacement vector in the respective directions of the coordinate axes x, y, z ; γ_x, γ_y – the unknown generalized angles of rotation of the normal sections of the plate in the planes xz and yz .

It can also be presented in the form [8]:

$$\begin{aligned} U(x, y, z) &= \sum_{n=0}^5 P_n u_n, (U, V; u, v); \\ W(x, y, z) &= \sum_{n=0}^4 P_n w_{n+1}, \end{aligned} \quad (2)$$

where $P_n = P_n(z/h)$ – Legendre polynomials; $\sigma_x, \sigma_y, \tau_{xy}$ – stress components [9].

Simultaneously, most of the authors of the proposed models of plate bending use a method of decomposing the displacement vector components into infinite power series along the transverse coordinate z' [10].

For a specific ordering of such expansions and a correct analysis of the level of refinement of the proposed bending theories [3] introduced such a concept as “energy consistency” between the functions of representing the components of the displacement vector, their number, the order of equations, and the number of boundary conditions to them. In particular, if we take only $n = 1$ in the expansions (2), the order of the calculated equations should be $p = 4 + 6n = 10$.

Simultaneously, within a formal approach, for the parameter $n = 3$, the system (2) will require integration by a 22nd-order equation. Therefore, without additional hypotheses, it is challenging to integrate such a system and satisfy the corresponding boundary conditions.

Different variants of physically correct models of two-dimensional shell and plate theories can be obtained using various approaches to minimize the weighted inconsistencies of such representations, which differ only in coefficients. To achieve this “consistency”, the authors propose to use specific variational methods of Lagrange, Castigliano, or Reissner [3, 4, 8]. The main disadvantage of such coherence is that their formal application leads to a significant increase in the order of differential equations and, consequently, a significant increase in the mathematical difficulty of obtaining solutions.

At the same time, the authors of [11, 12] showed how important the method of setting the boundary conditions and the influence of the degree of transverse anisotropy of

the material itself plays an essential role in obtaining reliable results.

In the papers [13, 14], a 3D system of homogeneous differential equations of motion of an anisotropic body in a cylindrical coordinate system and the corresponding boundary conditions within the framework of elasticity theory were constructed. The equations of motion and the boundary conditions allow us to consider layered anisotropic structures with variable thickness parameters.

Similar thorough studies were carried out in the research works [15, 16] for a multilayer cylindrical composite cantilever beam under its bending by a load at the ends and elastic axial tension-compression.

3 Research Methodology

For the case studies presented in [3, 11], the hypotheses of Ambartsumyan, Vlasov, and Reissner [17] were considered. Compared with other models, transverse compression was considered for studying the “energy consistency” effect and its helpfulness and disadvantages in practical applications.

Using solutions of well-known model problems, it was shown that in some cases of material anisotropy, a more accurate consideration of boundary conditions allows for obtaining results that cannot be obtained from standard generalized boundary conditions (e.g., for cases of slab support along the bottom edge, or for cylindrical surfaces pinching at the edges for a round one).

Lagrange’s variational principle for the total potential energy of an elastic system and several other assumptions also allows for obtaining similar equations for medium-thickness slabs of higher order. According to this principle,

$$\delta \tilde{\Pi} = \delta \Pi - \delta A, \quad (3)$$

where $\delta \Pi$ – variation of potential energy:

$$\begin{aligned} \delta \Pi &= \iint_S \int_{-h}^h [\sigma_x \delta \varepsilon_x + \sigma_y \delta \varepsilon_y + \sigma_z \delta \varepsilon_z + \\ &+ \tau_{xy} \delta \gamma_{xy} + \tau_{xz} \delta \gamma_{xz} + \tau_{yz} \delta \gamma_{yz}] dz dy dx; \end{aligned}$$

δA – variation of work of volumetric and surface forces:

$$\begin{aligned} \delta A &= \iiint_{V_p} (F_x \delta U + F_y \delta V + F_z \delta W) dV_p + \\ &+ \iint_S (q^- \delta \bar{W}^- + q^+ \delta \bar{W}^+) dS. \end{aligned}$$

Here, elements of slab volume dV_p and surface dS are introduced, as well as limit values of Naghdi approximation [18], used in determination of compression deformations:

$$\bar{W}(x, y, z) \simeq w(x, y) + z^2 w_2(x, y),$$

where q^\pm – corresponding values of the external load on the external surfaces $z = \pm h$ of the slab; F_x, F_y, F_z – projections of volumetric forces on the corresponding

coordinate axes, referred to the unit volume; $\varepsilon_x, \varepsilon_y, \varepsilon_z$ and $\gamma_{xy}, \gamma_{yz}, \gamma_{zx}$ – Cauchy dependencies.

After substituting into equation (1), instead of the deformations ε_i and γ_{ij} ($i = \{x, y, z\}$), through the Cauchy dependencies, the expressions for the displacements in the slab in the form of attracted series at the coordinate z (instead of infinite ones) [10]:

$$\begin{aligned} U(x, y, z) &= u(x, y) + \sum_{n=1}^3 u_n(x, y)z^n; \\ V(x, y, z) &= v(x, y) + \sum_{n=1}^3 v_n(x, y)z^n; \\ W(x, y, z) &= w(x, y) + \sum_{n=1}^4 w_n(x, y)z^n, \end{aligned} \quad (4)$$

where u, v, w – the displacements of the points of the slab center surface in the directions x, y , and z , respectively; u_n, v_n, w_n – arbitrary functions determined from the equilibrium equations of the slab element and the boundary conditions on its outer surfaces.

For integrating the expression for δII with the variable z , the expression for the variation of the potential energy due to internal forces can be obtained:

$$\begin{aligned} \delta \Pi &= \iint_S [\tilde{N}_x \delta(\frac{\partial u}{\partial x}) + \tilde{N}_y \delta(\frac{\partial v}{\partial y}) + N_{xy} \delta(\frac{\partial v}{\partial x} + \frac{\partial u}{\partial y}) + \\ &+ M_x \delta(\frac{\partial \gamma_x}{\partial x}) + M_y \delta(\frac{\partial \gamma_y}{\partial y}) + M_{xy} \delta(\frac{\partial \gamma_y}{\partial x} + \frac{\partial \gamma_x}{\partial y}) + \\ &+ Q_x \delta(\gamma_x + \frac{\partial \tilde{w}}{\partial x}) + Q_y \delta(\gamma_y + \frac{\partial \tilde{w}}{\partial y}) + \frac{4}{5} h^2 q_2 \delta w_2] dy dx, \end{aligned} \quad (5)$$

where the following expressions were introduced:

$$\begin{aligned} \tilde{w} &= w + \frac{1}{5} h^2 w_2; \\ q_1 &= 0,5(q^+ - q^-); \quad q_2 = q^- + q^+; \\ \tilde{N}_x &= N_x - 2hA_1 q_1; \quad \tilde{N}_y = N_y - 2hA_2 q_1; \\ \gamma_x &= \frac{3}{2h^3} \int_{-h}^h U z dz; \quad \gamma_y = \frac{3}{2h^3} \int_{-h}^h V z dz. \end{aligned}$$

The generalized angles of rotation γ_x and γ_y for the normal to the median surface of the slab can be rewritten as follows:

$$\{\gamma_x, \gamma_y\} = - \left\{ \frac{\partial \tilde{w}}{\partial x}, \frac{\partial \tilde{w}}{\partial y} \right\} + \frac{4}{5} \{\psi_x, \psi_y\},$$

where the following unknown functions have the nature of transverse shear deformations of the slab's median surface:

$$\begin{aligned} \tilde{w} &= w + h^2 w_2(x, y) = \tilde{W}^\pm; \\ \psi_x &= -3h^2 u_3; \quad \psi_y = -3h^2 v_3. \end{aligned}$$

The second term δA of the variational equation (5), in the absence of volumetric forces and with an accuracy of kh^2/a^2 can be reduced:

$$\delta A = \iint_S q_2 \delta \tilde{w} dS + \frac{4}{5} h^2 \iint_S q_2 \delta w_2 dS. \quad (6)$$

After choosing the unknown functions of displacements and angles of rotation $u, v, \tilde{w}, \gamma_x, \gamma_y$ as extremes in the variational equations (5), (6) and

considering the formulas for integration by parts, the variation operation $\delta \tilde{II}$ can be performed:

$$\begin{aligned} \delta \tilde{II} &= - \iint_S \left\{ \left(\frac{\partial \tilde{N}_x}{\partial x} + \frac{\partial N_{xy}}{\partial y} \right) \delta u + \left(\frac{\partial N_{xy}}{\partial x} + \frac{\partial \tilde{N}_y}{\partial y} \right) \delta v + \right. \\ &+ \left(\frac{\partial M_x}{\partial x} + \frac{\partial M_{xy}}{\partial y} - Q_x \right) \delta \gamma_x + \left(\frac{\partial M_{xy}}{\partial x} + \frac{\partial M_y}{\partial y} - Q_y \right) \delta \gamma_y + \\ &+ \left(\frac{\partial Q_x}{\partial x} + \frac{\partial Q_y}{\partial y} + q_2 \right) \delta \tilde{w} \} dy dx + \\ &+ \int_L [(N_{xn} - N_{xn}^*) \delta u + (N_{yn} - N_{yn}^*) \delta v + \\ &+ (M_{xn} - M_{xn}^*) \delta \gamma_x + (M_{yn} - M_{yn}^*) \delta \gamma_y + \\ &+ (Q_n - Q_n^*) \delta \tilde{w}] dL = 0, \end{aligned} \quad (7)$$

where L – the boundary of the contour S , $l = \cos(n, x)$, $m = \cos(n, y)$ – the directional cosines of the normal n to the contour S .

It also contains the following parameters:

$$\begin{aligned} Q_n &= Q_x l + Q_y m; \\ N_{xn} &= \tilde{N}_x l + N_{xy} m; \quad N_{yn} = N_{xy} l + \tilde{N}_y m; \\ M_{xn} &= M_x l + M_{xy} m; \quad M_{yn} = M_{xy} l + M_y m; \\ \{\tilde{N}_x, \tilde{N}_y\} &= \{N_x, N_y\} - 2h\{A_1, A_2\}q_1. \end{aligned}$$

The asterisked values in the contour integral (7) denote the forces acting on the contour of the plate. The following formula writes the expressions for internal forces and moments:

$$\begin{aligned} \{N_x, N_y, N_{xy}, Q_x, Q_y\} &= \int_{-h}^h \{\sigma_x, \sigma_y, \tau_{xy}, \tau_{xz}, \tau_{yz}\} dz; \\ \{M_x, M_y, M_{xy}\} &= \int_{-h}^h \{\sigma_x, \sigma_y, \tau_{xy}\} z dz; \\ M_x &= -D_1 \left(\frac{\partial^2 w_b}{\partial x^2} + \nu_{12} \frac{\partial^2 w_b}{\partial y^2} \right) - \\ &- \frac{4}{5} D_1 (1 - \nu_{12}) \frac{\partial^2 \Omega}{\partial x \partial y} + \bar{A}_1 q_2; \\ M_y &= -D_2 \left(\frac{\partial^2 w_b}{\partial y^2} + \nu_{21} \frac{\partial^2 w_b}{\partial x^2} \right) + \\ &+ \frac{4}{5} D_2 (1 - \nu_{21}) \frac{\partial^2 \Omega}{\partial x \partial y} + \bar{A}_2 q_2; \\ M_{xy} &= -2D_{66} \left[\frac{\partial^2 w_b}{\partial x \partial y} - \frac{2}{5} \left(\frac{\partial^2 \Omega}{\partial x^2} - \frac{\partial^2 \Omega}{\partial y^2} \right) \right]; \\ Q_x &= K_1 \left(\frac{\partial \tilde{w}_\tau}{\partial x} - \frac{\partial \Omega}{\partial y} \right); \quad Q_y = K_2 \left(\frac{\partial \tilde{w}_\tau}{\partial y} + \frac{\partial \Omega}{\partial x} \right); \\ \tilde{E}_1 &= \frac{E_1}{1 - \nu_{12} \nu_{21}}; \quad K_1 = \frac{4}{3} G_{13} h; \quad D_1 = \frac{2}{3} \tilde{E}_1 h^3; \\ w_b &= \tilde{w} - \frac{4}{5} \tilde{w}_\tau; \quad \tilde{w}_\tau = w_\tau - h^2 w_2(x, y); \\ D_{66} &= \frac{2}{3} G_{12} h^3; \quad A_1 = \frac{\nu_{31} + \nu_{32} \nu_{21}}{1 - \nu_{12} \nu_{21}}. \end{aligned} \quad (8)$$

The variations of the independent functions $u, v, \tilde{w}, \gamma_x, \gamma_y$, determining the displacements and generalized angles of rotation of the normal in the plate have arbitrary values everywhere except the contour. Consequently, all the factors near each of the variations of equation (7) should be equal to zero.

Therefore, by equating the coefficients near the independent variations to zero in the surface integral $\delta u, \delta v, \delta \tilde{w}, \delta \gamma_x, \delta \gamma_y$, a system of five differential

equations of equilibrium in forces for an orthotropic plate can be obtained:

$$\begin{aligned} \frac{\bar{E}_1}{G_{12}} \frac{\partial^2 u}{\partial x^2} + \frac{\partial^2 u}{\partial y^2} + (1 + \nu_{12} \frac{\bar{E}_1}{G_{12}}) \frac{\partial^2 v}{\partial x \partial y} &= 0; \\ \frac{\partial^2 v}{\partial x^2} + \frac{\bar{E}_2}{G_{12}} \frac{\partial^2 v}{\partial y^2} + (1 + \nu_{21} \frac{\bar{E}_2}{G_{12}}) \frac{\partial^2 u}{\partial x \partial y} &= 0; \end{aligned} \quad (9)$$

$$D_{66} \Delta \Omega + (D_1 - D_{16}) \frac{\partial^2 \Omega}{\partial x^2} = \frac{5}{4} K_1 \Omega, \quad \left(\begin{matrix} x \leftrightarrow y \\ 1 \leftrightarrow 2 \end{matrix} \right);$$

$$\begin{aligned} D_1 \frac{\partial^4 \tilde{w}}{\partial x^4} + 2D_{16} \frac{\partial^4 \tilde{w}}{\partial x^2 \partial y^2} + D_2 \frac{\partial^4 \tilde{w}}{\partial y^4} &= \\ = q_2 + (K_2 - K_1) \frac{\partial^2 \Omega}{\partial x \partial y} + \\ + \frac{4}{5} (D_1 \frac{\partial^4 \tilde{w}_\tau}{\partial x^4} + 2D_{16} \frac{\partial^4 \tilde{w}_\tau}{\partial x^2 \partial y^2} + D_2 \frac{\partial^4 \tilde{w}_\tau}{\partial y^4}) + \\ + (\bar{A}_1 \frac{\partial^2}{\partial x^2} + \bar{A}_2 \frac{\partial^2}{\partial y^2}) q_2; \end{aligned} \quad (10)$$

$$K_1 \bar{\Delta} \tilde{w}_\tau + (K_2 - K_1) \frac{\partial^2 \Omega}{\partial x \partial y} = -q_2;$$

$$\bar{\Delta} = \frac{\partial^2}{\partial x^2} + \frac{G_{23}}{G_{13}} \frac{\partial^2}{\partial y^2}.$$

After analyzing the resulting system of differential equations (9) and (10), it can be seen that it has a total 12th order. However, given that the last equation of system (10) is not decisive since the value of \tilde{w}_τ , can be expressed through the other values of the system (10) in the form (here for trans-tropic material):

$$K' \tilde{w}_\tau = -D \Delta \tilde{w} + \frac{2}{5} \left(\frac{E}{G'} + \frac{\nu''}{1 - \nu} \right) h^2 q_2.$$

Therefore, the independent system will be of the 10th order. Timoshenko's shear theory [6] (with the parameter $n = 3$) or Reissner's theory [17], which does not consider transverse compression at the plate bend.

Simultaneously, if approaching it formally, then system (8) is equivalent to the 22nd-order equations (without additional hypotheses) despite the contradictions regarding the order of the design equations.

The transverse compression through the dependence for W in the system (4) allows for new closed solutions to the problems of contact interaction of thin-walled structural elements, which adequately reflects the physical content of such problems.

Integration of the system of equations (9) and (10) requires the satisfaction of five boundary conditions at the edge of the slab. The equations for formulating the boundary conditions can be obtained by equating each of the components of the contour integral in the equation (7) to zero:

$$\begin{aligned} (N_{xn} - N_{xn}^*) \delta u &= 0; (N_{yn} - N_{yn}^*) \delta v = 0; \\ (Q_n - Q_n^*) \delta \tilde{w} &= 0; (M_{xn} - M_{xn}^*) \delta \gamma_x = 0; \\ (M_{yn} - M_{yn}^*) \delta \gamma_\varphi &= 0. \end{aligned} \quad (11)$$

Particularly, for slab edges $x = \text{const}$:

$$\begin{aligned} (\tilde{N}_x - N_x^*) \delta u &= 0; (N_{xy} - N_{xy}^*) \delta v = 0; \\ (Q_x - Q_x^*) \delta \tilde{w} &= 0; (M_x - M_x^*) \delta \gamma_x = 0; \\ (M_{xy} - M_{xy}^*) \delta \gamma_y &= 0. \end{aligned} \quad (12)$$

Based on the conditions (11), various boundary conditions at the slab edges can be generated. For example, to rigidly anchor a slab edge, the following five conditions should be met:

$$u = v = \tilde{w} = \gamma_x = \gamma_y = 0. \quad (13)$$

The conditions for hinging the edge of $x = \text{const}$ may vary. Examples of such conditions may include:

$$\begin{aligned} a) w = 0; \tilde{N}_x = N_{xy} = M_{xy} = M_x = 0; \\ b) w = v = \gamma_y = 0; \tilde{N}_x = M_x = 0. \end{aligned} \quad (14)$$

If the edge of $x = \text{const}$ is free of load ($N_x^* = N_{xy}^* = Q_x^* = M_x^* = M_{xy}^* = 0$), then the following homogeneous conditions can be obtained according to conditions (7):

$$\tilde{N}_x = N_{xy} = M_x = M_{xy} = Q_x = 0. \quad (15)$$

Thus, it can be argued that the theory describing the stress-strain state of a plate by equations (9), (10) and conditions (11), (13) obtained as a result of minimizing the Lagrange functional (7) is equivalent to the energy-consistent one ($n = 3$).

Simultaneously, it should be noted that neither the equilibrium equations nor the boundary conditions differ in form from the corresponding equations and conditions of plate theories obtained by other methods.

At the same time, the internal content of the elements of these dependencies differs significantly. For example, the displacement of the plate center surface w in applied theories such as Timoshenko's, a similar generalized displacement in Reissner's theory, and the averaged displacement \tilde{w} .

The same is true for other characteristics, such as generalized rotation angles γ_i or bending moments M_i . Simultaneously, as shown in [11], such generalizations of boundary conditions in displacements only at the level of the median surface can lead to less accurate results. Thus, it can be concluded that energy consistency optimizes the results within only a specific model (e.g., the Timoshenko model or the improved Ambartsumyan-Vlasov model [3]).

Considering formulas (8) and (10), the expressions for the stresses in the cross-sections of the slab can be obtained as dependencies on forces and moments:

$$\begin{aligned} \sigma_x &= \frac{N_x}{2h} + \frac{3M_x}{2h^3} z + \frac{\bar{E}_1}{K_1} \left(\frac{\partial Q_x}{\partial x} + \frac{\nu_{12}}{g} \frac{\partial Q_y}{\partial y} \right) f(z) + \\ &+ A_1 (\sigma_z - \sigma_0) + \tilde{\sigma}_x; \\ \sigma_y &= \frac{N_y}{2h} + \frac{3M_y}{2h^3} z + \frac{\bar{E}_2}{K_2} \left(\frac{\partial Q_y}{\partial y} + \nu_{21} g \frac{\partial Q_x}{\partial x} \right) f(z) + \\ &+ A_2 (\sigma_z - \sigma_0) + \tilde{\sigma}_y; \\ \tau_{xy} &= \frac{N_{xy}}{2h} + \frac{3M_{xy}}{2h^3} z + \\ &+ G_{12} \left(\frac{\partial \bar{Q}_x}{\partial y} + \frac{\partial \bar{Q}_y}{\partial x} + 2h^2 \frac{\partial^2 w_2}{\partial x \partial y} \right) f(z); \\ \tau_{xz} &= G_{13} (1 - z^2/h^2) \bar{Q}_x; \\ \tau_{yz} &= G_{23} (1 - z^2/h^2) \bar{Q}_y \end{aligned} \quad (16)$$

with the following parameters, functions, and features:

$$\begin{aligned}\tilde{\sigma}_x &= \tilde{E}_1 h^2 \left(\frac{\partial^2 w_2}{\partial x^2} + \nu_{12} \frac{\partial^2 w_2}{\partial y^2} \right) f(z); \\ \tilde{\sigma}_y &= \tilde{E}_2 h^2 \left(\frac{\partial^2 w_2}{\partial y^2} + \nu_{21} \frac{\partial^2 w_2}{\partial x^2} \right) f(z); \\ w_2 &= \frac{3 \alpha_z q_2}{8 E_3 h} - \frac{1}{2} \left(A_1 \frac{\partial \gamma_x}{\partial x} + A_2 \frac{\partial \gamma_y}{\partial y} \right); \\ \alpha_z &= 1 - (\nu_{13} A_1 + \nu_{23} A_2); \quad g = \frac{G_{23}}{G_{13}}; \\ f(z) &= \frac{z}{5} \left(1 - \frac{5z^2}{3h^2} \right); \quad \int_{-h}^h f(z) dz = \int_{-h}^h z f(z) dz = 0; \\ \sigma_0 &= q_1 + \frac{3z}{5h} q_2; \quad \sigma_z = q_1 + \frac{1}{4} \left(3 \frac{z}{h} - \frac{z^3}{h^3} \right) q_2; \\ q_1 &= \frac{1}{2} (q^+ - q^-); \quad q_2 = q^- + q^+; \\ \bar{Q}_x &= \frac{Q_x}{K_1}; \quad \bar{Q}_y = \frac{Q_y}{K_2}.\end{aligned}$$

The resulting formulas are the same as in [6], except for the terms that include the crimping function $w_2(x, y)$.

4 Results

4.1 Bending of a square transtropic slab hinged at the edges

To quantify these refinements for different slab models, we compare them with the exact solutions of the elasticity theory problem [3]. Let's consider the test bending problem for a square transtropic slab hinged at the edges ($x = [0, a]$, $y = [0, a]$) under the first condition (14) with a surface load $q^- = q_0 \sin \lambda x \sin \lambda y$ ($\lambda = \pi/a$), which varies in both directions of the outer surface according to the law of sine.

In this case, the displacement of the center surface and the normal stress σ_x in the center of the slab are found by the following formulas:

$$\begin{aligned}w^c &= \frac{q_0 a^4}{4\pi^4 D} (1 + 2\bar{\varepsilon}_1 \delta^2 - 4\bar{\varepsilon}_2 \delta^4); \\ \sigma_x^c &= \frac{3q_0 a^2 z}{8\pi^2 h^3} (1 + \nu) \left[1 + \frac{4\nu'' \delta^2}{5(1+\nu)} + \right. \\ &\quad \left. + \frac{\delta^2 R}{1-\nu^2} \left(\frac{z^2}{3h^2} - \frac{1}{5} \right) \right] - \frac{\nu'' q_0}{(1-\nu) 2},\end{aligned}\quad (17)$$

with the following parameters:

$$\begin{aligned}R &= \frac{E}{G'} - \nu''(3 + \nu) + \delta^2 \left(\frac{E}{E'} - r'A' \right); \\ \delta &= \lambda h; \quad \bar{\varepsilon}_{1,2} = \frac{\varepsilon_{1,2}}{(h^2, h^4)}; \quad r' = \frac{2E}{G'} + \nu''(3 - 2\nu).\end{aligned}$$

The calculations for the relative displacements $\bar{w} = wE/(2q_0h)$ of the middle surface and stresses $\bar{\sigma} = \sigma/q_0$ in isotropic and transtropic (GRP 27-63c) plates are given in Tables 1, 2, where the data are plotted for the relative thickness $2h/a = 1/3$ and equal Poisson's ratios $\nu = \nu'' = 0.3$.

Table 1 – Values of relative normal displacements \bar{w} and stresses $\bar{\sigma}$ in a slab for an isotropic material for equal Poisson's ratios $\nu = \nu'' = 0.3$

Parameter	Classical theory	3D model [3]	Reissner's theory [7]	The developed model
\bar{w}	2.27	3.49	3.48	3.50
$\bar{\sigma}$	1.78	2.12	1.87	2.15

Table 2 – Values of relative normal displacements \bar{w} and stresses $\bar{\sigma}$ in the slab for transtropic material for $E/E' = 3.1$ and $G/G' = 1.8$

Parameter	Reissner's model [15]	The developed model
\bar{w}	4.62	4.56
$\bar{\sigma}$	1.87	2.37

The data analysis in Tables 1 and 2 shows that using the Lagrange variational method and trimmed rows in the construction of refined bending theories for medium-thick plates is quite effective. The error margins of the constructed model in terms of displacements and stresses in the given test problem (isotropic material), compared to the 3D solution by Vlasov [16], are 0.2% and 1.2%, respectively. Errors in the classical theory are 35% and 16%, respectively.

The error margins of the theory of Reissner's theory ("energy consistent" for $n = 1$) in determining normal stresses are of the same order as in the classical Kirchhoff–Love theory, both for isotropic and transtropic materials.

The Timoshenko's theory, without considering the stress σ_z does not specify the values of normal stresses and gives the same results as the classical theory.

In Figure 1, using formula (15), graphs of changes in normal stresses $\sigma_x(0, z)/q_0$ in the central section of the slab ($x = a/2$; $y = b/2$) are plotted as a function of the thickness coordinate z , when the relative thickness of the slab is $2h/a = 1/3$.

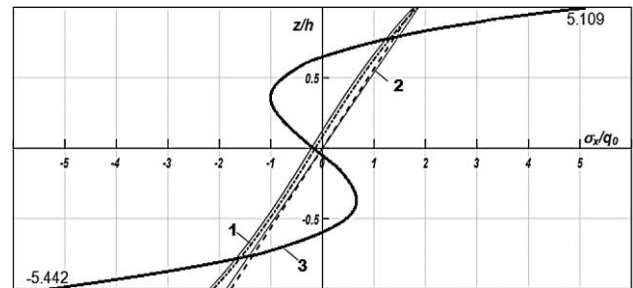


Figure 1 – Variation of normal stresses $\sigma_x(0, z)/q_0$ in the cross-section of the slab

Curves 1 (solid and dashed-dotted) were constructed for an isotropic material ($\nu = \nu'' = 0.3$) using formula (15) and according to the exact Vlasov's solution [16] to the spatial problem of elasticity theory, respectively.

The dashed and solid (next to each other) lines 2 are constructed according to a variant of Reissner's model

[14]. Also, the solid line (next to each other) refers to the solution of the classical Kirchhoff–Love theory.

These curves are very close for the isotropic case (with the same Poisson’s ratio) and for all other transtropic materials. Curve 3 was constructed for unidirectional graphite plastic with the following characteristics: $E/G' = 50$; $E/E' = 25$; $\nu = \nu'' = 0.25$.

Simultaneously, for an isotropic material, the curves of stresses with thickness obtained based on different plate models are approximately close to each other (Table 1, Figure 1). For graphite-plastics with low shear stiffness and transverse resistance, they are more than three times ($\sigma_x^1(0, -h) = -5.44q_0$ and $\sigma_x^2(0, -h) = -1.78q_0$) different from each other.

For example, curve 3, constructed for a plate made of unidirectional graphite plastic, changes the sign of the normal stress three times with thickness, while other models show only one change. This nature of the stress change results from the occurrence of quite significant self-balancing forces in the cross-sections of the plate, which are insignificant in isotropic plates but can occur in spatial bodies. The latter remarks on the results of the proposed plate model are confirmed by refined higher-order theories [14, 17] and numerical methods that incorporate edge effects more accurately.

Similar studies based on the equations of elasticity theory for an orthotropic material (without taking into account the stress σ_z and strain ε_z) were conducted in [17], where it is graphically shown that at a specific ratio E/G' , the stresses in the middle of the slab can exceed the stresses on its surface, as well as other differences.

4.2 Bending of a circular slab by a uniformly distributed load

Let’s consider the bending of a circular slab by a uniformly distributed load $q^- = q = \text{const}$, applied to the outer surface of the slab $z = -h$. The slab at the edge $r = a$ is rigidly clamped, and the boundary conditions (12) can be transposed to the following form:

$$u = 0; \tilde{w} = 0; \gamma_r = 0. \quad (18)$$

Simultaneously, for a broader consideration of the problem, we will write the boundary conditions, from which the previous ones can be derived, in the form:

$$u = 0; W|_{z=z_0} = 0; (\partial U/\partial z)|_{z=z_{0u}} = 0. \quad (19)$$

Here, the parameters z_0 and z_{0u} are the distances from the center surface of the slab in the positive direction of the z axis, where the corresponding displacements or rotation angles are assumed to be zero.

For example, at $z_{0u} = \pm h/\sqrt{5}$ and $z_0 = 0$, the condition (12) can be obtained. Under these conditions, the solution to the problem [10] was obtained and, particularly, the formula for the normal stress σ_r , including the parameter z_{0u} affecting the value σ_r is as follows:

$$\sigma_r(r, z) = \frac{3(1+\nu)qa^2z}{32h^3} \left[1 - \frac{(3+\nu)r^2}{(1+\nu)a^2} + \tilde{\eta} \frac{h^2}{a^2} + \frac{4h^2}{(1-\nu)a^2} (\tilde{m}_1 + \tilde{m}_2 \frac{z^2}{h^2}) \right] - 0,5A'q, \quad (20)$$

where the following parameters were introduced:

$$\alpha = \frac{\nu''G'}{2G}; \tilde{\eta} = \frac{8(1-\alpha)}{1-\nu} \left(\frac{1}{5} - \frac{z_{0u}^2}{h^2} \right) \frac{G}{G'};$$

$$\tilde{m}_1 = -\frac{2G}{5G'} + \frac{\nu''(11+\nu)}{5(1+\nu)}; \tilde{m}_2 = \frac{2G}{3G'} - \frac{\nu''(3+\nu)}{3(1+\nu)}.$$

In the Reissner’s theory [7], the parameters $\tilde{\eta}$, \tilde{m}_1 , and \tilde{m}_2 are equal to zero, although it can also be considered “energy consistent”.

Table 3 shows the results of calculating the stresses σ_r in a slab according to formula (17), the relative thickness of which $h/a = 1/5$, and the Poisson’s ratios $\nu = \nu'' = 0.25$.

Table 3 – Dimensionless stress values $\tilde{\sigma}_r(\mathbf{0})$ and $\tilde{\sigma}_r^*(a)$

$\tilde{\sigma}_i$	z	3D classical theory [18]	$z_{0u} = 0$ (18)	$z_{0u} = \pm h/\sqrt{5}$ (18)	$z_{0u} = \pm h$ (17)
$\frac{\sigma_r}{q}$	$-h$	<u>-3.63</u> -2.93	<u>-3.63</u> -5.29	<u>-3.41</u> -4.08	<u>-3.63</u> 0.80
	h	<u>3.21</u> 2.93	<u>3.29</u> 4.96	<u>3.08</u> 3.74	<u>3.33</u> -1.13
$\frac{\sigma_r^*}{q}$	$-h$	<u>5.94</u> 4.69	<u>5.05</u> 6.72	<u>4.84</u> 4.50	<u>5.09</u> 8.42
	h	<u>-5.87</u> -4.69	<u>-5.39</u> -7.05	<u>-5.17</u> -5.84	<u>-5.42</u> -8.75

The effect on the values of radial stresses $\tilde{\sigma}_r(\mathbf{0})$ and $\sigma_r^*(a)$ of the method of clamping by changing a particular parameter z_{0u} is investigated. The values in the denominator (in bold) are obtained for a transversally isotropic material ($E/E' = 2$; $G/G' = 5$).

The results calculated by the formula (17) are compared with the corresponding results (third column) obtained in the formulation of the spatial problem of elasticity theory by the method of determinant states (numerator) and the classical Kirchhoff–Love theory (in the denominator).

From the analysis of the data in Table 3, it can be concluded that in the case of an isotropic material, the boundary conditions (12) obtained from the contour integral (5) lead to less accurate results compared to the three-dimensional solution, as well as other cases of pinching: $z_{0u} = 0$; $z_{0u} = \pm h$.

Simultaneously, in the case of the transtropic material in the last column ($z_{0u} = \pm h$), the results obtained in the center of the slab differ even in sign compared to the case of an isotropic material. It is obvious that the component $\tilde{\eta}$, which partially describes the self-equilibrium stress state, is much higher than the component from the moment stress state. It is clear that such “anomalies” require additional verification by performed calculations of the spatial problem or by experimental data.

Special attention, when calculating slabs of medium thickness, requires an assessment of the effect of the corrections for the consideration of the transverse compression strain ε_z and transverse normal stress σ_z in

the model equations, as well as in the calculation formulas for displacements and stresses.

The multiplier denotes the above corrections in formulas (15) and (18) ν'' (Poisson's ratio). Equating it to zero, we obtain formulas where only the correction for the transverse shear strain is valid.

For the Timoshenko's and the Ambartsumyan's theories, where these corrections are not considered, the normal displacement $\bar{w} = 3.69$ (for a thickness of $a/(2h) = 3$). This result has an error of about 6%.

The magnitude of the effect of the transverse compression strain is characterized by the difference in displacements of the outer surfaces (upper and lower), which also depends on the value of the modulus ratio E/E' . In particular, in this case, the displacement of the upper and lower surfaces will be 3.60 (3.56) and 3.15 (3.19), i.e. 6–10%. The errors in calculating normal stresses for this problem will be approximately the same. Simultaneously, for transtropic materials, at large modulus ratios E/E' , the errors (together with the consideration of the transverse shear strain) can be relatively large, as observed for the case of a round slab.

At the same time, it should be noted that in the first problem for a rectangular slab, the above effects were not observed due to the specificity of the given load, where the boundary conditions on the side surfaces were satisfied at all points of the edges.

However, when considering transverse compression under some loads – the contact interaction of beams and slabs with rigid dies - there is no question of a quantitative assessment of contact pressure because even qualitative information is not preserved.

For example, the problem of forced bending of a rod along a predetermined surface (Figure 2) was considered by Tymoshenko in the formulation of hypotheses of the classical Bernoulli–Euler rod bending theory, where contact pressure was generally considered absent.

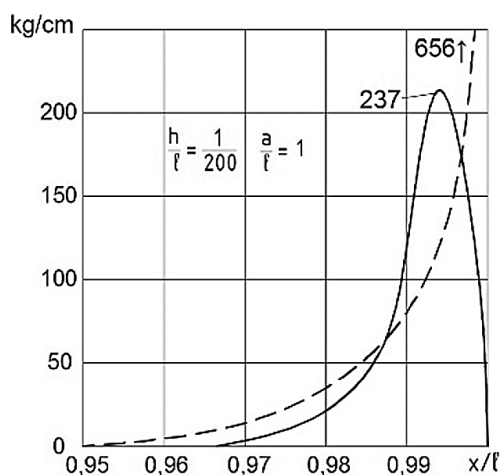


Figure 2 – Distribution of contact pressure in a long rod

5 Discussion

In a refined formulation, considering transverse shear deformations, the problem was first solved by Filonenko–Borodich [3]. It gives a numerical example for a steel strip with a length of $2l = 0.2$ m, width $t = 0.01$ m, and thickness $2h = 0.001$ m, pressed against the rigid base of the pattern by concentrated forces applied to its ends (Figure 2).

The radius of curvature of the pattern base $R = 1$ m. It was necessary to determine the magnitude of the forces applied to the strip to bend it according to a given pattern and investigate the nature of the pressure distribution on the strip.

According to the Filonenko–Borodich approach, the solution to the problem considering only the effect of the transverse shear strain (Figure 2) is dashed. However, according to the solution given in this article, the magnitude of these forces is $P' = 339$ N. The maximum pressure reached at the ends of the strip $q_{max} = 65.6$ MPa.

The results obtained by using the corresponding formulas (Figure 2, solid line) give the following values for the maximum forces and maximum pressure: $P' = P/2 = 252$ N; $q_{max} = 23.7$ MPa.

The numerical analysis of formulas presented in [19] shows that the pattern's response to the strip is concentrated near its ends in areas of size about $a = 0.02$ m. The rest of the pattern is practically free of load.

The periodic problem of bending an infinite strip with dies based on the equations of plane elasticity theory was also considered most consistently and thoroughly by Kier and Silva [20], where the size of the contact area could be both large and relatively small. The solution was constructed in trigonometric series and reduced to pairwise integral equations that were solved numerically. A similar method was used by other authors [3] without considering the sticking effect.

A similar problem, but for a beam partially supported on a rigid base, was checked in the formulation of a plane problem of elasticity but by the boundary element method. The difference between the numerical results and those obtained using the formulas did not exceed 3 %.

6 Conclusions

The article considers the problem of construction and accuracy of “energy-consistent” models of medium-thickness slabs. Using the examples of solutions for one of these models, numerical results are presented for a rectangular slab hinged on a hinge and a circular slab clamped on the edge of the slab, made of isotropic and transtropic materials. The contact interaction of rigid objects with elastic elements (beams, slabs) is considered. The influence of a particular refinement on the nature of the stress state of a particular structural element is investigated. The calculated results are compared with the corresponding available results obtained in the formulations of the three-dimensional problem of elasticity and the classical Kirchhoff–Love theory.

Each numerical example for the constructed bending model played a particular role in the considered refinements at different loads and boundary conditions. The first example shows that, provided that the boundary conditions are exactly satisfied, the numerical results for normal stresses in an isotropic slab coincide with the results of the spatial problem to within 1 %. At the same time, the data obtained for slabs made of composite materials can differ significantly from both the spatial problem for an isotropic material and the classical results. That is, there is a problem with three-dimensional results for composite slabs.

The analysis of the comparisons shows that the accuracy of a particular model depends mainly on the level

and perfection of the proposed hypotheses and only then on the correctness of their use and the application of variational methods in the construction and integration of the resulting differential equations. This is especially true for models for slabs of medium thickness made of anisotropic materials when edge effects can extend to the entire slab volume, leading to a change in the signs of stresses on the outer surfaces (the second problem). Using the example of the problem of forced bending of a rod, it was shown that any slab model that does not consider transverse compression cannot give a correct solution even in the first approximation, so such problems should be solved only if available.

References

1. Ghugal, Y. M., Shipi, R. P. (2002). A refined shear deformation theories of isotropic and anisotropic laminated plates. *Journal of Reinforced Plastics*, Vol. 21(9), pp. 775–813. <https://doi.org/10.1177/073168402128988481>
2. Lo, K. N., Christensen, R. M., Wu, E. M. (1977). A high-order theory of plates deformation. Part 1. Homogeneous plates. *J. Appl. Mech.*, Vol. 44(4), pp. 663–668. <https://doi.org/10.1115/1.3424154>
3. Shvabyuk, V. I., Rotko, S. V., Shvabyuk, V. V. (2022). *Mathematical Models of Deformation of Composite Plates and Beams: Contact Interaction with Dies and Bases*. Influence of Cracks. Vezha-Druk, Lutsk, Ukraine.
4. Grigorenko, Y. M., Grigorenko, A. Y., Vlaikov, G. G. (2009). *Problems of Mechanics for Anisotropic Inhomogeneous Shells on Basis of Different Models*. Lutsk National Technical University, Lutsk, Ukraine.
5. Shvabyuk, V. I., Rotko, S. V. (2015). *Linear Deformation, Strength and Stability of Composite Shells of Medium Thickness*. Lutsk National Technical University, Lutsk, Ukraine.
6. Timoshenko, S. P., Woinowsky-Kriger, S. (1959). *Theory of Plates and Shells*. McGraw-Hill, New York, NY, USA.
7. Reissner, E. (1947). On bending of elastic plates. *Quarterly of Applied Mathematics*, Vol. 5(1), pp. 55–68.
8. Zelensky, A. G., Prusakov, O. P., Vovchenko, M. G. (1999). A variant of the nonclassical bending theory of transversally isotropic plates and gentle shells. *Bulletin of the Dnipro State University. Series "Mechanics"*, Vol. 2(2), pp. 58–65.
9. Reissner, E. (1953). On a variational theorem for finite elastic deformations. *Journal of Mathematics and Physics*, Vol. 32(1–4), pp. 129–135. <https://doi.org/10.1002/sapm1953321129>
10. Kilchevskiy, N. A. (1965). *Fundamentals of the Analytical Mechanics of Shells*. National Aeronautics and Space Administration, Washington, DC, USA.
11. Shvabyuk, V. I., Rotko, S. V., Fedorus, V. Y., Shvabyuk, V. V. (2021). Influence of transverse anisotropy and type of boundary conditions on the stress state of a circular transtropic plate. *Strength of Materials*, Vol. 53, pp. 440–448. <https://doi.org/10.1007/s11223-021-00304-z>
12. Srinivas, S., Rao, A. K., Joga Rao C. V. (1969). Flexure of simply supported thick homogeneous and laminated rectangular plates. *ZAMM*, Vol. 49(8), pp. 449–458. <https://doi.org/10.1002/zamm.19690490802>
13. Pagano, N. J. (1969). Exact solutions for composite laminates in cylindrical bending. *Journal of Composite Materials*, Vol. 3(3), pp. 398–411. <https://doi.org/10.1177/002199836900300304>
14. Semenuk, M. P., Trach, V. M., Podvornyi, A. V. (2023). Stress–strain state of a thick-walled anisotropic cylindrical shell. *International Applied Mechanics*, Vol. 59, pp. 79–89. <https://doi.org/10.1007/s10778-023-01201-5>
15. Kovalchuk, S. B., Goryk, A. V. (2018). Elasticity theory solution of the problem on bending of a narrow multilayer cantilever with a circular axis by loads at its end. *Mechanics of Composite Materials*, Vol. 54, pp. 605–620. <https://doi.org/10.1007/s11029-018-9768-y>
16. Kovalchuk, S. B., Gorik, A. V., Pavlikov, A. N., Antonets, A. V. (2019). Solution to the task of elastic axial compression–tension of the composite multilayered cylindrical beam. *Strength of Materials*, Vol. 51, pp. 240–251. <https://doi.org/10.1007/s11223-019-00070-z>
17. Reissner, E. (1975). On transverse bending of plates, including the effect of transverse shear deformation. *International Journal of Solids and Structures*, Vol. 11(5), pp. 569–573. [https://doi.org/10.1016/0020-7683\(75\)90030-X](https://doi.org/10.1016/0020-7683(75)90030-X)
18. Lisitsyn, B. M. (1970). Calculation of pinched plates in the formulation of a spatial problem of the theory of elasticity. *Applied Mechanics*, Vol. 6(5), pp. 18–23.
19. Naghdi, P. M. (1957). On the theory of thin elastic shells. *Quarterly of Applied Mathematics*, Vol. 14(4), pp. 369–380.
20. Keer, L. M., Silva, M. A. G. (1970). Bending of a cantilever brought gradually into contact with a cylindrical supporting surface. *International Journal of Mechanical Sciences*, Vol. 12(9), pp. 751–760. [https://doi.org/10.1016/0020-7403\(70\)90050-0](https://doi.org/10.1016/0020-7403(70)90050-0)